Supporting information

Nanofibrous polymeric beads from aramid fibers for efficient bilirubin removal

Zihang Peng,[a] Ye Yang,[a] Jiyue Luo,[a] Chuanxiong Nie,[a,*] Lang Ma ,[a] Chong Cheng,[a,b] Changsheng Zhao[a,c,*]

[a] College of Polymer Science and Engineering, State Key Laboratory of Polymer Materials Engineering, Sichuan University, Chengdu 610065, China

[b] Department of Chemistry and Biochemistry, Freie Universitat Berlin, Takustr. 3, 14195 Berlin, Germany

[c] National Engineering Research Center for Biomaterials, Sichuan University, Chengdu 610064, China

* Corresponding author. Tel: +86-28-85400453, Fax: +86-28-85405402, E-mail:

(C. X Nie) Chuanxiong_Nie@163.com.; (C.S. Zhao) zhaochsh70@163.com or zhaochsh70@scu.edu.cn

Endothelial cell culture: Human umbilical vein endothelial cells (HUVECs) were grown in R1640 medium supplemented with 10% fetal bovine serum (FBS) (Hyclone, USA), 2 mM L-glutamine and 1 *vol.* % antibiotics mixture (10,000 U penicillin and 10 mg streptomycin). Cultures were maintained in a humidified atmosphere of 5% CO_2 at 37 °C (Queue Incubator, Paris, France). Confluent cells were detached from the culture flask with sterilized PBS and 0.05% trypsin/EDTA solution. The culture medium was changed every day.

Live/dead cell staining: The HUVECs were seeded onto the samples at a density of approx. 2.5×10^4 cells/cm^2. The cells cultured in the wells without samples served as the control in this study. After 2 days of culture on the different substrates, the Live/dead staining was performed as described in an earlier study. To stain with FDA/PI, 0.1 mL of FDA working solution and 0.03 mL of PI were added directly to the culture medium. The cells were stained for 3 min at room temperature, and then washed with PBS. The cells were then immediately visualized by fluorescence microscopy (DMIRE2, Leica). FDA fluorescence was monitored by excitation with an argon-laser (excitation wavelength 492 nm, emission wavelength 520 nm); whereas PI positively charged samples were excited with a helium-neon-laser (excitation wavelength 537 nm, emission wavelength 566 nm). The average numbers of the ECs adhered on the material surfaces were estimated from at least 6 fluorescence images.

MTT assay: After cell culture for 2, 4 and 6 days, the viability of the HUVECs was determined by an MTT assay. 45 μL of the MTT solution (1 mg/mL in the test medium) was added to each well and incubated for 4 h at 37 °C. Mitochondrial dehydrogenases of viable cells selectively cleave the tetrazolium ring, yielding blue/purple formazan crystals. 400 μL of ethanol was added to dissolve the formazan crystals. Therefore, the quantity of the formazan crystals dissolved in the ethanol reflects the level of cell metabolism. The dissolved solution was shaken homogeneously for about 15 minutes. The solution of each sample was aspirated into

a microtiter plate and the optical density of the formazan solution was read on a Microplate reader (Model 550, Bio-Rad) at 492 nm. All the experiments were repeated twelve times, and the results were expressed as means ± SD.

Adsorption kinetics study. The pseudo-first-order equation, also known as the Lagergren rate equation, was the first rate equation for the adsorption of liquid-solid system based on solid capacity and it can be represented in the following form:[1]

$$\ln(q_e - q_t) = lnq_e - k_1 t \quad (1)$$

where q_t (mg/g) is the bilirubin adsorption amount at time t (min); q_e (mg/g) stands for the bilirubin adsorption amount at the equilibrium; k_1 is the rate constant of pseudo-first-order equation. The plots of $ln(q_e\text{-}q_t)$ against t give a straight line with $-k_1$ as slope and lnq_e as intercept, as shown in Figure S1(A).

The parameters for the pseudo-first-order equation are shown in Table S1. The calculated q_e values for Kev, Kev_9-CNT_1, Kev_5-CNT_5 and PES were 48.36, 51.28, 59.37 and 3.85 mg/g, respectively, which were bigger than the experimental ones. The correlation coefficients (r^2) of bilirubin adsorption for Kev, Kev_9-CNT_1, Kev_5-CNT_5 and PES were 0.990, 0.989, 0.996 and 0.986, respectively, which indicated that the experimental data agreed with this model.

The pseudo-second-order equation based on adsorption equilibrium capacity was also used. It can be expressed in the following form:[2]

$$\frac{t}{q_t} = \frac{1}{k_2 q_e^2} + \frac{t}{q_e} \quad (2)$$

where k_2 is the rate constant of pseudo-second-order equation. q_t, q_e and t have the same meaning as those in pseudo-first-order equation. From the slope and intercept of the plot of t/q_t versus t in Figure S1(B), the k_2 and q_e values for the beads can be obtained. As seen in Table S1, the calculated values for the Kev, Kev_9-CNT_1, Kev_5-CNT_5 and PES were much higher than the experimental values. Meanwhile, the q_e obtained from the pseudo-first-order model was closer to the experimental data, which indicated that the pseudo-first-order model was more suitable for explaining the

kinetics for the adsorption of bilirubin onto the beads.

The intraparticle diffusion model was used to further identify the adsorption mechanism, considering the pseudo-first-order and the pseudo-second-order models could only help in identifying the adsorption process. The intraparticle diffusion equation is characterized in the following form:[3]

$$q_t = k_p t^{1/2} + C \quad (3)$$

where k_p is the rate constant of intraparticle diffusion model; q_t (mg/g) is the bilirubin adsorption amount at time t (min); C is a constant for any experiment (mg/g).

According to this model, the curves with two steps were obtained by plotting q_t *vs* $t^{1/2}$, indicating that during the adsorption process the intraparticle diffusion was involved. As shown in Figure S1(C), the rate constants could be calculated by the slope of the linear part of each curve, and the intercept C could also be obtained from the extrapolation of the first step in the curve to time axis.[4]

The parameters of intraparticle diffusion model for the bilirubin adsorption by the beads are summarized in Table S2. The two linear sections with different slopes of each curve indicated that two rate-limited steps occurred during the adsorption process. As indicated by other researchers,[5, 6] the first linear section was attributed to the external surface adsorption or diffusion in the macro-pores of the beads until the exterior surface reached the saturation, whereas the second one was involved with the intraparticle diffusion. Thus, diffusion in the macro-pores was the dominant factor at the initial period while the intraparticle diffusion controlled the adsorption rate then.

Table S1. The parameters of pseudo-first model and pseudo-second model for adsorption of bilirubin by the beads.

Samples	$q_{e(exp)}$	**Pseudo-first-order**			**Pseudo-second-order**		
	(mg/g)	k_1 (g/mg.min)	$q_{e(cal)}$ (mg/g)	r^2	k_2 (g/mg.min)	$q_{e(cal)}$ (mg/g)	r^2
Kev	42.91	0.0197	48.36	0.990	0.0002	69.44	0.955
Kev$_9$-CNT$_1$	48.15	0.0254	51.28	0.989	0.0002	73.75	0.967
Kev$_5$-CNT$_5$	57.16	0.0289	59.37	0.996	0.0004	74.68	0.982

PES	3. 01	0.0141	3.85	0.986	0.0016	6.06	0.923

Table S2. The parameters of intraparticle diffusion model for the adsorption of bilirubin by the beads.

Samples	**C** (mg/g)	**Step Ⅰ**		**Step Ⅱ**	
		k_1 (mg/g $min^{1/2}$)	r_1^2	k_2 (mg/g $min^{1/2}$)	r_2^2
Kev	-5.93	4.7837	0.974	2.0447	0.991
Kev_9-CNT_1	-4.65	5.2651	0.983	1.1507	0.976
Kev_5-CNT_5	-0.78	6.3639	0.995	0.7043	0.990
PES	-0.984	0.9736	0.996	0.0663	0.990

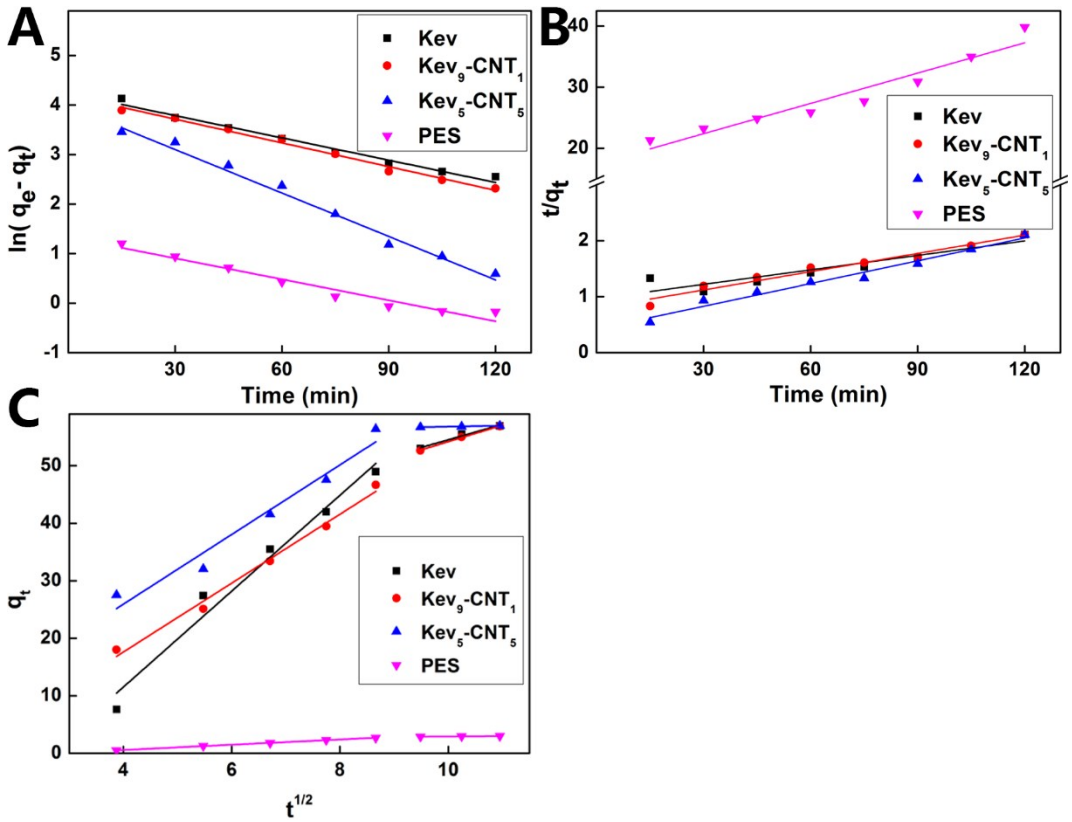

Figure S1. (A) Application of pseudo-first-order adsorption model for the adsorption of bilirubin. (B) Application of pseudo-second-order adsorption model for the adsorption of bilirubin. (C) Application of intraparticle diffusion model for the adsorption of bilirubin.

Figure S2. Dispersion of the beads in water.

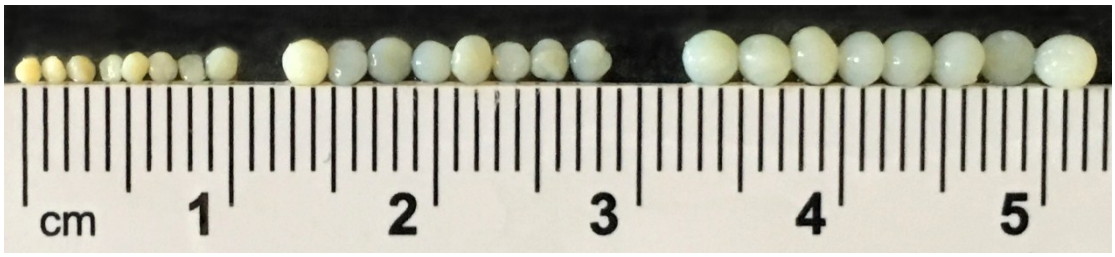

Figure S3. The beads with different sizes, which were prepared by injecting the Kevlar nanofiber solution into ethanol.

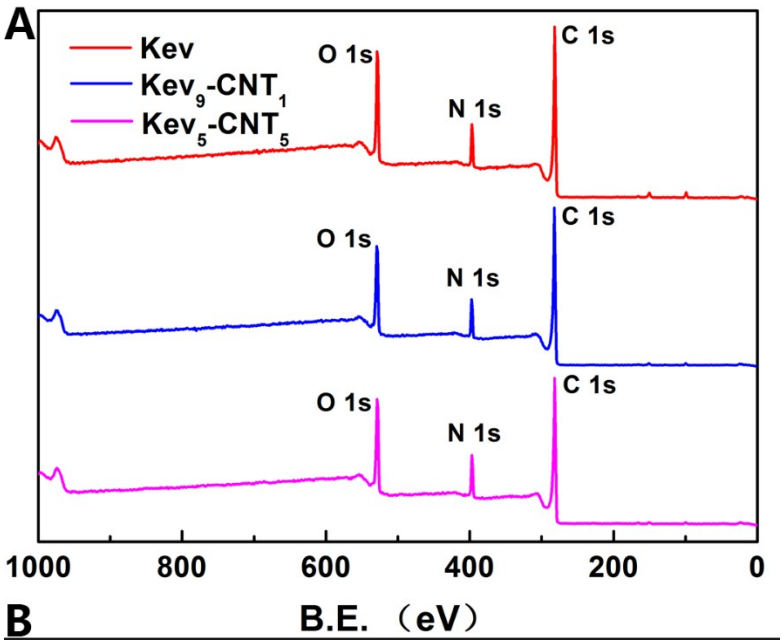

B

Samples	Element analysis (at.%)		
	O	C	N
Kev	16.31	75.75	7.94
Kev_9-CNT_1	14.96	77.41	7.63
Kev_5-CNT_5	10.23	84.90	4.87

Figure S4. (A) XPS wide spectra for the beads. (B) Element analysis for the beads, which were estimated from XPS wide spectra.

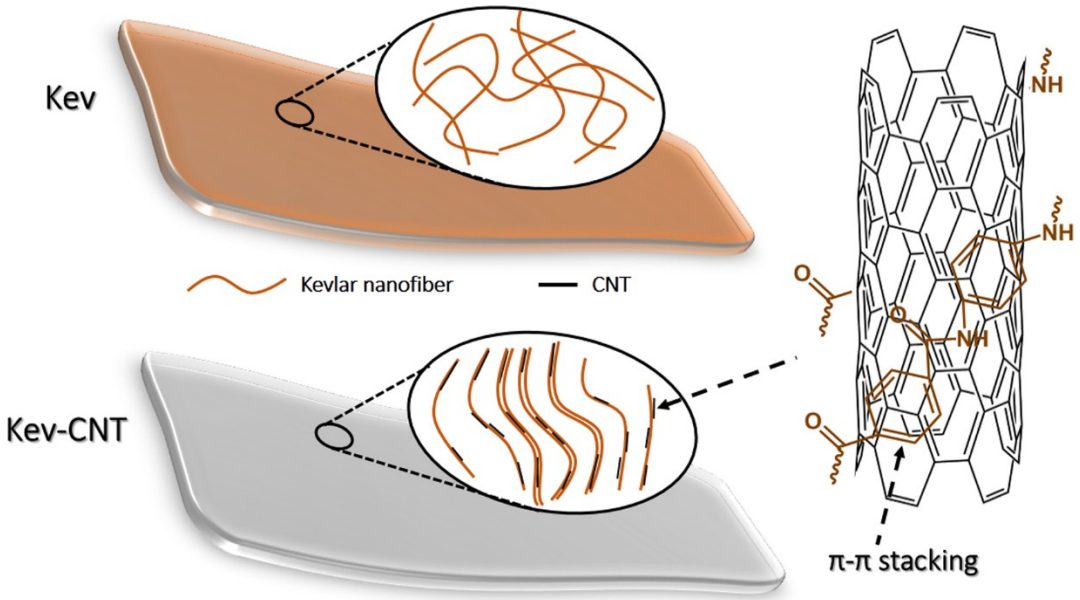

Figure S5. Alignment of CNTs in Kevlar matrix. After adding CNT, the composite

solution became more insoluble in ethanol and thus accelerated the phase separation process, leading to the formation of layered structure instead of porous structure.

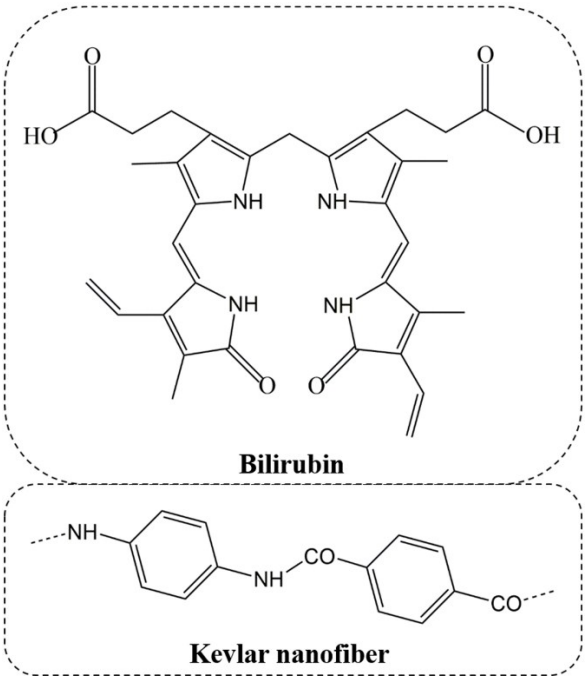

Figure S6. The structures of bilirubin and Kevlar nanofiber.

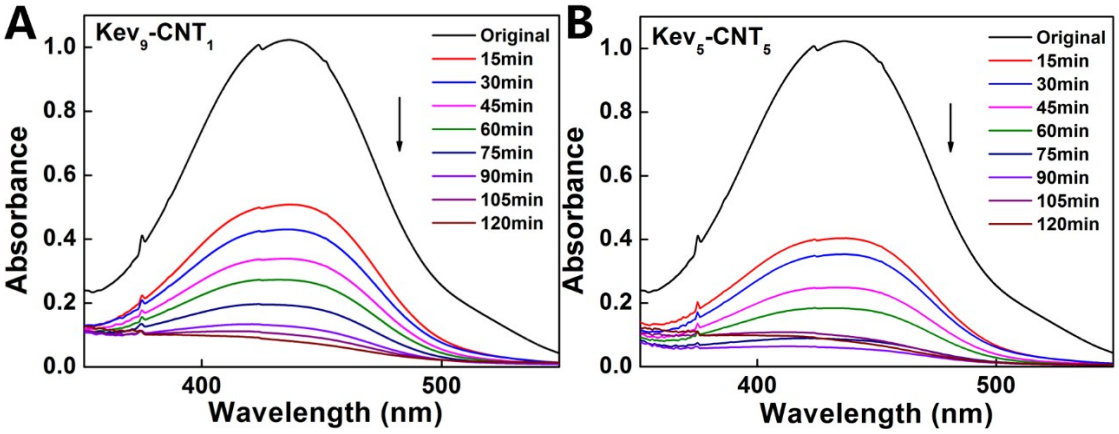

Figure S7. UV-vis adsorption spectra during bilirubin adsorption within 120 min.

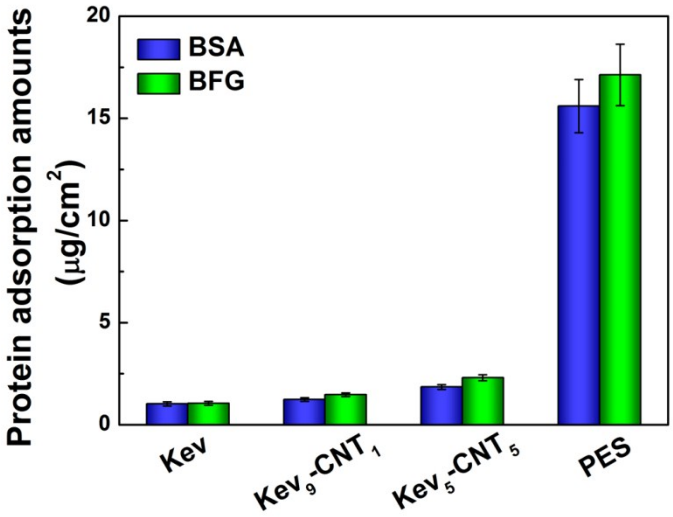

Figure S8. The protein adsorption amounts for the beads, which are expressed as μg/cm^2. Note that the results were estimated according to N_2 sorption results.

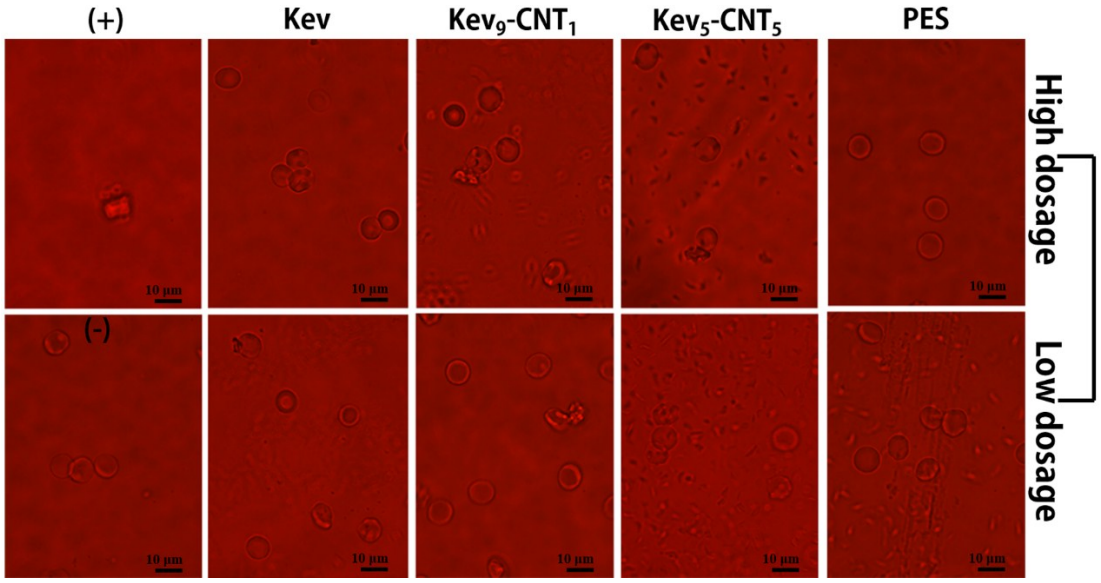

Figure S9. RBC morphologies after contacting with the samples.

References

1. L. H. V. Thanh and J. C. Liu, *Ind. Eng. Chem. Res.*, 2013, 53, 1242-1248.
2. G. Zelmanov and R. Semiat, *Desalination*, 2014, 333, 107-117.
3. M. Doğan, Y. Özdemir and M. Alkan, *Dyes Pigments*, 2007, 75, 701-713.
4. C. S. Cheng, J. Deng, B. Lei, A. He, X. Zhang, L. Ma, S. Li and C. Zhao, *J. Hazard. Mater.*, 2013, 263 Pt 2, 467-478.
5. S. J. Allen, G. Mckay and K. Y. Khader, *Environ. Pollut.*, 1989, 56, 39-50.
6. K. G. Bhattacharyya and A. Sharma, *Dyes Pigments*, 2005, 65, 51-59.